



HAL
open science

A study to constrain the geometry of an active fault in southern Italy through borehole breakouts and downhole logs.

Simona Pierdominici, Maria Teresa Mariucci, Paola Montone

► To cite this version:

Simona Pierdominici, Maria Teresa Mariucci, Paola Montone. A study to constrain the geometry of an active fault in southern Italy through borehole breakouts and downhole logs.. *Journal of Geodynamics*, 2011, 52 (3-4), pp.279. 10.1016/j.jog.2011.02.006 . hal-00780027

HAL Id: hal-00780027

<https://hal.science/hal-00780027>

Submitted on 23 Jan 2013

HAL is a multi-disciplinary open access archive for the deposit and dissemination of scientific research documents, whether they are published or not. The documents may come from teaching and research institutions in France or abroad, or from public or private research centers.

L'archive ouverte pluridisciplinaire **HAL**, est destinée au dépôt et à la diffusion de documents scientifiques de niveau recherche, publiés ou non, émanant des établissements d'enseignement et de recherche français ou étrangers, des laboratoires publics ou privés.

Accepted Manuscript

Title: A study to constrain the geometry of an active fault in southern Italy through borehole breakouts and downhole logs.

Authors: Simona Pierdominici, Maria Teresa Mariucci, Paola Montone



PII: S0264-3707(11)00042-1
DOI: doi:10.1016/j.jog.2011.02.006
Reference: GEOD 1049

To appear in: *Journal of Geodynamics*

Received date: 27-9-2010
Revised date: 15-2-2011
Accepted date: 19-2-2011

Please cite this article as: Pierdominici, S., Mariucci, M.T., Montone, P., A study to constrain the geometry of an active fault in southern Italy through borehole breakouts and downhole logs., *Journal of Geodynamics* (2010), doi:10.1016/j.jog.2011.02.006

This is a PDF file of an unedited manuscript that has been accepted for publication. As a service to our customers we are providing this early version of the manuscript. The manuscript will undergo copyediting, typesetting, and review of the resulting proof before it is published in its final form. Please note that during the production process errors may be discovered which could affect the content, and all legal disclaimers that apply to the journal pertain.

1 **A study to constrain the geometry of an active fault in southern Italy through borehole**
2 **breakouts and downhole logs.**

3

4 Simona Pierdominici¹, Maria Teresa Mariucci¹ and Paola Montone¹

5

6 ¹ Istituto Nazionale di Geofisica e Vulcanologia, Sezione di Sismologia e Tettonofisica, via di
7 Vigna Murata, 605, Rome, Italy

8

9 Submitted to: Journal of Geodynamics

10

11

12 Corresponding author:

13 Simona Pierdominici

14 Istituto Nazionale di Geofisica e Vulcanologia

15 Via di Vigna Murata 605

16 00143 Rome, ITALY

17 Tel: +39-06-51860576

18 Fax: +39-06-51860507

19 E-mail address: simona.pierdominici@ingv.it

20

20 Abstract

21 Identification of an active fault and the local versus regional present-day stress field in the
22 Irpinia region (southern Apennines) have been performed along a 5900m deep well (San Gregorio
23 Magno 1) by a detailed breakout and geophysical log analysis. The selected area is characterized by
24 diffuse low magnitude seismicity, although in historical times moderate to large earthquakes have
25 repeatedly struck it. On 23rd November 1980 a strong earthquake ($M=6.9$) nucleated on a 38km-long
26 normal fault, named Irpinia fault, producing the first unequivocal historical surface faulting ever
27 documented in Italy. The analysis of stress-induced wellbore breakouts shows a direction of
28 minimum horizontal stress $N18^{\circ}\pm 24^{\circ}$, fairly consistent with the regional stress trend ($N44^{\circ}\pm 20^{\circ}$).
29 The small discrepancy between our result and the regional stress orientation might be related to the
30 influence of local stress sources such as variations of the Irpinia fault plane orientation and the
31 presence of differently oriented active shear zones. This paper shows for the first time a detailed
32 analysis on the present-day stress along a well to identify the Irpinia fault at depth and constrain its
33 geometry.

34
35 Key words: Borehole breakout, geophysical log, present-day stress field, seismogenic fault,
36 southern Apennines, Italy.

38 1. Introduction

39 This paper is mainly devoted to the present-day stress field study performed in a high seismic
40 hazard area of southern Italy (Cinti et al., 2004; Faenza and Pierdominici, 2007) in order to assess a
41 methodology to identify and constrain active faults at depth along deep wells.

42 The present-day stress state can be assessed by different techniques, including the analysis of:
43 (i) borehole breakouts, (ii) focal mechanism solutions, (iii) exposed active fault segments, (iv) well
44 cores, and (v) crustal deformation and differential strain (Ding and Zhang, 1991; Zoback, 1992;
45 Seto et al., 1998). Breakouts are used as indicators of the direction of maximum and minimum

46 horizontal stress (S_{Hmax} and S_{Hmin} , respectively) and correspond to observation points along deep
47 wells (Bell and Gough, 1979; Zoback et al., 1985). Many studies have shown that the present-day
48 stress orientation in a region is quite homogeneous and independent of the stratigraphy and depth
49 (e.g. Plumb and Cox, 1987; Castillo and Zoback, 1994), whereas along a borehole the breakout
50 orientations can change due to the presence of active faults (Barton and Zoback, 1994; Wu et al.,
51 2007). As reported by several authors stress perturbations have been associated to open fractures
52 and to active faults which have slipped recently (Bell et al., 1992; Shamir and Zoback, 1992; Barton
53 and Zoback, 1994; Mariucci et al., 2002; Wu et al., 2007). Moreover, shear zones at depth usually
54 show physical properties different from the nearby undamaged rock and downhole logs can record
55 these features.

56 In this paper we have analysed the present-day stress along and around a deep well and tried to
57 identify at depth some shear zones and the seismogenic fault, named Irpinia, located in the southern
58 Apennines. This fault is related to the 1980 $M_s=6.9$ Irpinia earthquake, and represents the first
59 unequivocal surface faulting ever documented in Italy. Its geometry is not well constrained by
60 geophysical exploration and aftershock data analysis because this tectonic structure is relatively a
61 young fault that has not yet developed enough cumulated vertical slip to be clearly resolved by
62 seismic reflection profiles (Pantosti and Valensise, 1993; Improta et al., 2003; Cippitelli, 2007;
63 Patacca, 2007; Figure 1). This paper shows for the first time a detailed analysis on the present-day
64 stress nearby the seismogenic fault in the context of the overall setting. The Irpinia fault trace is
65 located ~ 1.3 km westward from the well San Gregorio Magno 1 (herein named SGM1), and
66 according to its geometry, the well should cut off it. If this is true, the main observation of Barton
67 and Zoback, (1994) that stresses reorient close to faults should be verified. The idea is to study the
68 present-day stress in the SGM1 well to identify the possible stress perturbations close to the Irpinia
69 fault. Then, borehole breakouts, downhole log data and tectonic structures along the deep well
70 SGM1 have been analysed.

71

72 **2. Geological-structural setting and regional seismicity**

73 The southern Apennine belt is part of the Alpine orogens of the Mediterranean area,
74 developing from the interaction between the converging Africa-Apulian and European plates since
75 Late Cretaceous time, (e.g. D'Argenio et al., 1973; Dewey et al., 1989; Mazzoli and Helman, 1994
76 and references therein; Butler et al., 2004). The southern Apennines are a NE-verging fold-and-
77 thrust belt that began to grow mainly since the lower Miocene (Bonardi et al., 1988; Patacca et al.,
78 1990) due to deformation of the Adriatic subducting margin. The thrust belt is characterized by
79 allochthonous units derived from both carbonate platform and pelagic basin successions (Apenninic
80 Platform and Lagonegro Basin, respectively), which are stratigraphically overlain by Neogene
81 foredeep and wedge-basin deposits (Miocene and Pliocene successions). These units are completely
82 detached from their original substratum and transported onto the foreland sequence of the Apulian
83 carbonate Platform (e.g. Doglioni et al., 1996; Mazzoli et al., 2004).

84 In the early Pliocene (Scandone et al., 2003), the entire pile of nappes overthrusts the Apulian
85 carbonate platform giving rise to a complex duplex system (e.g., Mostardini and Merlini, 1996;
86 Cello et al., 1987, 1989; Casero et al., 1988; Ascione et al., 2003; Patacca and Scandone, 2007). In
87 this tectonic context, the thrust sheet emplacement moved following the opening of the Tyrrhenian
88 back-arc basin (Patacca et al., 1990) as a consequence of the roll-back of the subducting Adriatic
89 plate (Malinverno and Ryan, 1986; Doglioni, 1991). Only in the middle-late Pliocene, the Apulia
90 Platform underwent shortening processes that created duplexing in the deep-seated carbonates and
91 displacement of the overlying allochthonous sheets (Patacca and Scandone, 2007). The processes of
92 thrusting and Adriatic-verging nappe transport have been active on the eastern side until the lower
93 part of middle Pleistocene (Casero et al., 1988; Patacca et al., 1990; Roure et al., 1991; Cinque et
94 al., 1993; Pieri et al., 1997; Patacca and Scandone, 2001), when the flexure-hinge retreat in the
95 Adriatic plate suddenly stopped (Patacca and Scandone, 2007).

96 For further information on the geological and structural setting, the reader is referred to the wide
97 existing literature (e.g., Casero et al., 1991; Patacca and Scandone, 1989; 2004; Lavecchia, 1988;
98 Pescatore et al., 1999; Galadini et al., 2000; Giano et al., 2000; Lentini et al., 2002; Valensise and
99 Pantosti, 2001; Schiattarella et al., 2003; Scrocca et al., 2007).

100 Concerning the seismicity, the southern Apennines are characterized by recent low magnitude
101 seismic events, punctuated by large historical earthquakes that shook the area in the past (CPTI
102 Working Group, 2004) (Figure 2). Strong historical events ($I_0=IX-X$) have been well documented
103 since 1500: 1561-Vallo di Diano; 1694-Irpinia; 1826-Tito; 1831-Rivello; 1836-Lagonegro; 1851-
104 Basilicata; 1857-Val d'Agri; 1930-Irpinia; 1980-Irpinia (Esposito et al., 1988; Marturano et al.,
105 1988; Porfido et al., 1988; CPTI Working Group, 2004).

106 The instrumental seismicity, recorded by the Istituto Nazionale di Geofisica e Vulcanologia
107 (INGV) since 1981 is characterized by magnitudes generally lower than 4.0 (Castello et al., 2008).
108 Only a few isolated seismic sequences hit the southern Apennines in the last years (Figure 2, Table
109 1). In 1990-1991 the Potenza area was shaken by a seismic sequence ($M_w=5.7$ and $M_w=5.2$) which
110 occurred from about 2 to 25km depth with the mainshocks showing E-W dextral strike-slip
111 mechanism (Azzara et al., 1993; Ekström, 1994; CPTI Working Group, 2004; Di Luccio et al.,
112 2005); in 1996 the Irpinia area was hit by a seismic sequence characterized by normal faulting
113 mechanisms with a mainshock ($M_w=5.1$) at 8km depth (Cocco et al., 1999; Cucci et al., 2004); in
114 1998 normal faulting earthquakes occurred in the north Pollino area with $M_w=5.6$ (Michetti et al.,
115 2000; Pondrelli et al., 2002) and in 2002 the Melandro-Pergola basin was affected by $M_w=4.1$
116 earthquake at a depth of 9km (Cucci et al., 2004; Frepoli et al., 2005). The seismicity is mainly
117 placed along the axial part of the belt, within the shallow crust, showing NE-SW T-axes with
118 prevailing normal faulting focal mechanisms (Gasparini et al., 1985; Frepoli and Amato, 2000;
119 Pondrelli et al., 2006; Maggi et al., 2009 among many others). As mentioned above, this trend is
120 also coherent with the active stress field (Figure 2) inferred from geological and borehole breakout
121 data (e.g., Amato et al., 1995; Montone et al., 2004).

122

123 **2.1 The 1980 M6.9 Irpinia earthquake**

124 In the last century, the most important and largest seismic event in the southern Apennines was
125 the Irpinia earthquake that occurred on November 23, 1980 with $M_s=6.9$ (Boschi et al., 1993). It
126 was one of the most disastrous events in Italy, causing the death of about 3000 people and the total
127 destruction of 15 towns within a radius of nearly 50km. This earthquake nucleated at a depth of 10-
128 12km (Westaway and Jackson, 1987) with a focal mechanism characterized by NW-SE normal
129 faulting planes and by a moment tensor of $2,4 \cdot 10^{19}$ Nm (Giardini, 1993) (Figure 3a). The aftershock
130 distribution indicated that the area of the earthquake source was about $14 \times 40 \text{ km}^2$ providing also
131 information on source geometry (Deschamps and King, 1980; Amato and Selvaggi, 1993) and on
132 the relationship between crustal structure and faulting mechanism (Chiarabba and Amato, 1994;
133 Improta et al., 2003). However, the 3D locations from local earthquake tomography did not allow
134 constraining the fault geometry at depth accurately (Deschamps and King, 1984).

135 The Irpinia earthquake consists of three subevents, at 0s (the mainshock), at ~20s and ~40s from
136 the mainshock (Bernard and Zollo, 1989). Associated to the 0s and 20s events, a 38km long rupture
137 at the surface was partially recognized by Westaway and Jackson (1984) and then totally defined by
138 Pantosti and Valensise (1990). Its mean strike is $N308^\circ$, with a 60° - 70° dip to the northeast with an
139 average value of normal slip of 61cm along the fault (Pantosti et al., 1993) and a total vertical throw
140 of about 50m in the last 150krs (Ascione et al., 2003; Improta et al., 2003). Pantosti and Valensise
141 (1990, 1993) divided the 1980-surface rupture into 3 main segments on the basis of geological and
142 geomorphological observations of the scarp, which is clearly linked to the coseismic deformation at
143 depth. These 3 scarp strands are, from northwest to southeast: the Cervialto, the Marzano-Carpineta
144 and the San Gregorio Magno (Figure 3a), separated by two surface faulting gaps (the Sele and the
145 San Gregorio Magno gap). The first shock (at 0 sec) is associated both to the Marzano-Carpineta
146 segment and to the Cervialto scarp (approximately 8-10 km long). The second event happened after
147 20s along a 8km San Gregorio Magno segment. Considering only seismological data, the last event

148 (40s) is supposed to be located on an antithetic, SW-dipping branch fault (Ofanto fault segment)
149 (Improta et al., 2003) in front of the Cervialto and Marzano-Carpineta structures (Figure 3a); no
150 evidence of surface rupture exists for this event.

151

152 **3. San Gregorio Magno 1 well**

153 **3.1 Stratigraphy and structural outline**

154 The SGM1 well is located at 797m elevation near the Marzano-Carpineta fault scarp (Figure
155 3b). It was drilled by British Gas RIMI in 1996-1997 down to a depth of 5900m with the goal of
156 reaching a structural high in the Apulia carbonate Platform, which is generally a target of the oil
157 industry in the southern Apennines, imaged by commercial and deep reflection profiles (Patacca
158 and Scandone, 2007)) and gravity data modelling (Improta et al., 2003). The SGM1 well (Patacca,
159 2007) crossed three main tectonic units bounded by two thrust faults at 2280 m and 3377 m and
160 different lithological units (Figure 4a).

161 According to Patacca (2007), the well penetrates 2280m of the Mesozoic carbonates of the
162 Alburno-Cervati Unit (part of the Apenninic carbonate Platform succession), ~1100m of the
163 Lagonegro Unit II (part of Lagonegro basinal succession) and ~2600m of the Apulian carbonate
164 Platform. The first Unit is composed of: i) “lime breccias” (early Cretaceous-Jurassic), typical of
165 slope environments and characterized by calcirudites and calcarenites, and ii) Dolomia Principale
166 Formation (late Triassic), deposited in a tidal flat environment and characterized by dolomites and
167 dolomitic limestones. The underlying Lagonegro Unit II, deposited in a deep-marine basin, consists
168 of: i) the Galestri Formation (early Cretaceous), that is mainly formed of claystones and shales and
169 subordinate calcilutites and calcarenites; ii) the Scisti Silicei Formation (Jurassic to Rhaetian),
170 containing calcarenites and radiolarites and subordinate siliceous shales (2735-3070m), and in the
171 lower part claystones and shales with subordinate calcarenites and calcilutites (3070-3200m);
172 finally iii) the M. Facito Formation (early-middle Triassic), formed by shales, sandstones, siltstones
173 and siliciclastic calcarenites, subordinate radiolarites and limestones. The deepest tectonic unit, the

174 Apulia, includes: “wildflysch” (middle Miocene to early Pliocene), siciliaclastic flysch deposits
175 derived from the Apennines nappes deposited in foredeep basin; Gessoso Solifera Formation
176 (Messinian) characterized by anhydrites and evaporitic limestones, typical of evaporitic carbonate
177 ramp; “lime breccias” (upper Cretaceous) typical of slope environment consisting of calcarenites,
178 calcilutites and calcirudites; “shallow-water carbonates” (Dogger-upper Cretaceous) deposited in a
179 shelf environment. Besides the two thrusts, following the reconstruction of Patacca (2007), the well
180 also encountered a system of SW-dipping normal faults at 440m and 3198m (Figure 4a). As the
181 surface rupture of the Irpinia fault is located ~1.3km westward from the well, according to its
182 geometry (N308° striking, 60°-70° northeast dipping), the borehole should intersect the fault within
183 the depth range ~2300-3800m (Figure 4a). As a matter of fact, the fault has not been unequivocally
184 recognized from the available data, either on stratigraphic logs or on seismic profiles. As mentioned
185 in the introduction, one possible explanation is that the relatively young fault has not yet developed
186 enough cumulated vertical slip to be clearly resolved by seismic reflection profiles (Pantosti and
187 Valensise, 1993; Improta et al., 2003; Cippitelli, 2007; Patacca, 2007). For this reason we have
188 jointly used different methods, including borehole breakouts and downhole logs, to identify the
189 possible active shear zones and the Irpinia fault.

190

191 **3.2 Borehole breakout data**

192 Method

193 Borehole breakout analysis is an important tool for the evaluation of stress patterns in the
194 uppermost crust (Bell and Gough, 1979; Zoback and Zoback, 1980, 1991; Zoback et al., 1985,
195 1989; Plumb and Cox, 1987). Breakouts fill the gap between data from earthquake focal
196 mechanisms and surface measurements (e.g. active faults, extensional fractures and strain release
197 measurements): they are the result of localized conjugate compressive shear failures that develop
198 along deep wells in an anisotropic stress field with a triangular shape in cross-section. The shear
199 planes are tangential to the circumference of the borehole and identify breakout zones parallel to the

200 direction of the S_{hmin} . The first breakout develops in the borehole very soon after the passage of the
201 drill bit and continues to propagate along the axis of the borehole and into the formation (Bell and
202 Gough, 1983). Mechanisms that explain the formation of these features have been extensively
203 examined in the literature (Babcock, 1978; Bell and Gough, 1979; Zoback et al., 1985; Haimson
204 and Heirrick, 1986; Zheng et al., 1989; Amadei and Stephansson, 1997).

205 Borehole breakouts are identified from four-arm caliper readings collected routinely with
206 conventional dipmeter logging tools. Different borehole geometries are defined as: i) “in-gauge”, if
207 the hole has the dimensions of the drill bit called bit size; ii) “breakout zone”, when one diameter is
208 elongated and the orthogonal one has the bit size dimension; iii) “key seat”, when the drill-string
209 wear causes a pear-shaped borehole with an artificial elongation at the low side of the well. It
210 occurs when the borehole is highly deviated from vertical; iv) “washout”, an enlargement of the
211 borehole in an “over-gauge hole” (Plumb and Hickmann, 1985). To obtain the average direction and
212 standard deviation of the least horizontal stress in the well, the statistical method from Mardia
213 (1972) has been applied in this study. Results are shown as rose diagrams scaled by length, and a
214 quality factor is assigned to each well (from A=highest quality to E=lowest quality) according to the
215 criteria used for the World Stress Map (Heidbach et al., 2008), first suggested by Zoback (1992).

216

217 Analysis

218 The breakout analysis of SGM1 well has been performed by four-arm caliper log data from
219 1200m to 5900m depth with two gaps (2645-2945m and 4775-4950m). The results of the
220 investigation showed: a) key seats between 1200 and 2000 m; b) no breakout between 5585 and
221 5900 and c) breakouts between 2000 and 5585m.

222 The result of the entire well shows a cumulative breakout length of 675m with an average S_{hmin}
223 orientation of $N18^\circ$ and a standard deviation of 24° (Figure 4h), with a data quality C (according to
224 World Stress Map criteria; Heidbach et al., 2008).

225 A more detailed breakout analysis, considering all the data quality, has been performed for each
226 lithological and tectonic unit to understand the scattering of breakout data (Figure 4d, f, g and Table
227 2). We have identified a breakout zone from 2000 to 2075m in the Dolomia Principale (belonging to
228 the Alburno-Cervati tectonic unit) N348° oriented for a 75m total length. The Lagonegro II tectonic
229 unit is characterized by a S_{hmin} orientation N38°±33° and a length of 365m with five breakout zones
230 related to: the Galestri Fm. with S_{hmin} N310° oriented and a total length of 125m; the Scisti Silicei
231 Fm. N41° and a total length of 165m, and the M. Facito Unit with S_{hmin} N33° trending and 75m long.
232 The Apulia tectonic unit is characterized by a S_{hmin} orientation N7°±28° for a total length of 607m:
233 in the Wildflysch S_{hmin} is N325° oriented (total length of 245m) and in the Shallow-water carbonate
234 unit is N15° (total length of 362m) (Table 2). No breakouts have been found in the Gessoso Solfifera
235 and Lime Breccias units.

236 As the regional stress field is well constrained in the area (S_{hmin} N44°±20°) (Montone et al., 1997;
237 Montone et al., 2004), we believe it is possible to distinguish, along the well, anomalous stress
238 directions departing from the regional trend and associate them with shear zones intersected by the
239 drilling (Shamir and Zoback, 1992; Barton and Zoback, 1994; Wu et al., 2007). Barton and Zoback
240 (1994) point out that the stress field rotates in proximity to an active fault due to small slip
241 increments on the fault, possibly induced by the tectonic movement or due to an increase of pore
242 pressure on the fault when drilling through it. With the purpose of identifying the Irpinia fault, the
243 stress field detected from SGM1 has been compared to the regional stress orientation. Any
244 deviation from the regional value has been considered as a local rotation of the stress field - if the
245 breakout orientation deviates from the regional one more than 15° - and is shown as clockwise or
246 anticlockwise rotation (Figure 4e). Along the SGM1 well, anomalously oriented breakouts occur in
247 five intervals: 2000m-2650m, 3450m-3855m, 4350-4560m, around 4800m and around 5500m
248 (Figure 4d-e).

249 As observed in other deep wells, when the breakout trend abruptly changes it is possible to identify
250 faults and/or fracture zones otherwise difficult to recognize by seismic reflection data and drill

251 cutting analysis (Bell et al., 1992). We have distinguished four zones that separate different
252 breakout orientations (Figure 4): from 2650m to 2950m (zone 1), 3275m to 3450m (zone 2), 3855m
253 to 4320m (zone 3), and 5057m to 5460m (zone 4).

254 Considering the uncertainty of the fault geometry, three of the anomalous zones (zone 1, 2 and
255 3) are located around the area where the well is supposed to crosscut the Irpinia fault: in fact
256 according to most authors (e.g., Boschi et al., 1981), the Irpinia fault has a dip between 60° to 70°
257 corresponding to a depth of intersection with SGM1 approximately between 2300m to 3800m
258 (Figure 4).

259

260 **4. Breakout versus downhole geophysical data**

261 The stress field along the SGM1 well has been studied using two approaches. First, we have
262 analysed the borehole breakout data to obtain information on the present-day stress field. Second, we
263 have used these data and the downhole logs to identify possible shear zones and the Irpinia fault
264 itself. Shear zones at depth usually show physical properties different from the nearby undamaged
265 rock and these features can be recorded by downhole logs. As by now observed in other drilled
266 active faults (Wu et al., 2007; Wu et al., 2008) the shear zones correspond to the most significant
267 changes in sonic and resistivity curves with respect to their average trend at depth.

268 Assuming the SGM1 well crossed the Irpinia fault we have analyzed three downhole curves
269 (gamma ray, resistivity and sonic; Figure 5) in order to detect their anomalous physical properties
270 with respect to overall value characterizing each lithology. For our analysis we have used an
271 extremely detailed stratigraphic log (courtesy of Etta Patacca and Paolo Scandone) that allowed us to
272 recognize and discard the anomalies related to the small-scale lithological variations and to the
273 identified faults. In fact, according to this interpretation those faults are westward dipping, whereas
274 the Irpinia fault dips toward east.

275 The remaining sectors showing significant changes in downhole logs are located at the
276 following depths (Figure 5): around 2350m (sector A), around 3100m (sector B) with two small

277 areas, around 3800m (sector C), around 4300m (sector D) and around 4700m (sector E). Considering
278 the Irpinia fault geometry (60° - 70° dipping) we can exclude the two deepest sectors (D and E).
279 Particularly, in the sector A the sonic curve shows a decrease with respect its mean value (Figure 5)
280 while the other curves do not seem to show any anomaly; in sector B we have identified two small
281 zones showing anomalous peaks in all the curves (a decrease in gamma ray and sonic logs and an
282 increase in resistivity, Figure 5). Finally, in sector C we have identified a well defined peak showing
283 an increase in the sonic curve and a decrease in the resistivity curve trend (Figure 5). All these
284 sectors correspond to washout zones (Figure 5b) that also support the presence of shear zones. In
285 fact, when a borehole crosses a highly fractured area, the stress concentration enhances the effect of
286 natural fractures that are mechanically weaker, and can easily produce collapse of the wellbore wall,
287 detected as enlargements of the borehole size. Only sectors A and C are located within the
288 previously identified five anomalous breakout intervals, whereas sector B is located where breakouts
289 are consistent with the regional S_{hmin} orientation. As mentioned before, abrupt breakout rotations
290 indicate the presence of active shear zones. For this reason we suggest that the Irpinia fault is located
291 around 2350m (sector A) or around 3800m (sector C). In both zones we have more confident data
292 revealing not only abrupt breakout rotations (\sim NW-SE oriented) but also washout presence,
293 geophysical log anomalies not directly connected to the lithology, and consistency with the fault dip
294 deduced from focal mechanisms and surface data.

295

296 **5. Discussion and conclusion**

297 The stress analysis has allowed us to constrain the S_{hmin} orientation along the well ($N18^{\circ}\pm 24^{\circ}$),
298 suggesting that it is moderately consistent with the neighbouring regions (Figure 6). The slight
299 difference between the regional stress field ($S_{hmin} = N44^{\circ}\pm 20^{\circ}$) and the achieved SGM1 S_{hmin} is due
300 to the presence of \sim N-S S_{hmin} orientations in the deepest part of the well, mainly within the Apulia
301 tectonic unit (Figure 4g and Figure 6). In Figure 6 breakouts are shown as rose diagrams instead of
302 average S_{hmin} orientations; in fact we believe that the average S_{hmin} orientations are more appropriate

303 for regional tectonic reconstructions, whereas for local tectonic interpretations it is preferable to
304 consider rose diagrams, where it is easier to resolve the contribution of possible different
305 orientations within the same well.

306 Two main directions are observable not only in SGM1 but also in other breakout solutions (even
307 of higher quality, A or B) along the belt and the foredeep. A ~N-S orientation has been recognized
308 also in another deep well located in the northern part of the Irpinia area (Figure 6) and could be
309 linked to the presence of ~E-W tectonic structures or to the changing trend of the NW-oriented
310 faults. Actually, it is a common feature of a fault plane showing variable orientations that can
311 correspond to slight deviations in the local principal stress orientations. The inferred S_{hmin} orientation
312 is not exactly at 90° with respect to the $N308^\circ$ Irpinia fault mean direction, but it is fairly consistent
313 with the “zig-zagging” trend of the fault (Pantosti and Valensise, 1993) and with the local tectonic
314 structures displaying ~E-W directions (Caiazza et al., 1992; Ascione et al., 2003). In detail, in this
315 area there is interference between the $N150^\circ$ and $N110^\circ$ - 100° trends relative to the Marzano-
316 Carpineta structure and Mt. Ognà fault respectively, both reactivated during the late Quaternary
317 (Ascione et al., 2003).

318 Concerning seismological data, in correspondence of the Irpinia area a lot of earthquake focal
319 mechanisms (Cocco et al., 1999; Cucci et al., 2004; Frepoli et al., 2005; Maggi et al., 2009) exhibit
320 both normal faulting and strike slip mechanisms (Figure 6). Particularly, the fault plane solutions
321 closer to the well clearly show ~N-S oriented T-axis, on ~E-W nodal planes (Figure 6 and Table 1,
322 solutions from 20 to 23), which fit the deepest results of the breakout analysis.

323 Then, we hypothesize that the localized stress rotations along the SGM1 well probably result
324 from slip on nearby faults indicating active deformation in the crust. Also the geophysical logs
325 show significant anomalies in the physical properties in correspondence of two hypothesized major
326 active shear zones: at 2350m (sector A) and around 3800m (sector C), depths where we suppose the
327 Irpinia fault is located.

328 Then, we propose some possible hypotheses in terms of general geometry of the Irpinia fault,
329 especially concerning its dip, segmentation or continuity (Figure 7). Starting from the information
330 that the fault dips 60° at 10-12km depth, as inferred from the focal mechanism solution of the 1980
331 Irpinia earthquake, and taking into account the lower and upper bounds of the surface fault dip (60°
332 and 70°) we obtain four different options. If the well crosses the fault in the sector A (i.e. the fault
333 dip is around 60°) we can suppose: 1) a straight fault plane 60° dipping from surface to focal depth
334 (red line in Figure 7); or 2) a fault plane changing dip from 70° at surface to 60° immediately below
335 (blue line in Figure 7). Whereas, if sector C is the true hole-fault intersection (i.e. fault dip around
336 70°) we can have: 3) an irregular fault plane trend (like a “vertical segmentation”) with two dip
337 changes, from 60° to 70° at few kilometres from the surface and from 70° to 60° around 10 km; or 4)
338 a 70° dipping fault changing to 60° down to focal depth (yellow line in Figure 7). The first two
339 hypotheses (numbers 1 and 2) differ only for the dip at surface and then can be considered as one
340 hypothesis. Among these different hypotheses we believe that the number 3 is the less reliable
341 considering its geometry and also it is very similar to the hypothesis number 4 at depth. Then we
342 concentrate on the last hypothesis that agrees with the fault geometry proposed by Amato and
343 Selvaggi (1993) based on the seismicity distribution and earthquake focal mechanisms. Occurrence
344 of the fault in sector C is also consistent with the idea of stress decoupling due to the Irpinia fault, as
345 supported by breakout orientations along the well that show a prevailing \sim NNE-SSW direction
346 (immediately below sector C) and \sim NS in the deepest part of the well (4300-5600m; Figure 4, rose
347 plot of column f). We believe that this sector has a slightly higher degree of probability, with respect
348 to sector A, to be the real location of Irpinia fault along SGM1 well and then, the yellow line the
349 most probable geometry of the fault (Figure 7).

350 The identification of fault geometry is an important factor for the characterization of the seismic
351 behaviour and therefore the seismic hazard assessment of an area. The seismic behaviour of a fault
352 can be considered both in space and in time. In the first case, the location and the geometry of the
353 active faults influence the interactions with the surrounding faults that may accumulate stress or

354 initiate. This observation is consistent with substantial release of accumulated strain energy during
355 earthquakes and a redistribution of stress in adjacent areas (e.g., Marzocchi et al., 2009). In the
356 second case, the seismic behaviour of a fault is studied by examining the historical seismicity and
357 the paleoseismological records to estimate recurrence intervals along different fault segments.
358 In this paper, the most significant result is that using downhole log and borehole breakout data is
359 possible to constrain the most likely location of an active fault at depth.

360

361

362 **Acknowledgement**

363 This work was partially funded by the Italian Ministry of University and Research in the framework
364 of Project FIRB “Research and Development of New Technologies for Protection and Defense of
365 Territory from Natural Risks”, W.P. C3 “Crustal Imaging in Italy”, coordinated by P. Montone.
366 Many thanks are due to the reviewers for their precious suggestions which greatly improved the
367 paper.
368

369 **References**

- 370 Amadei, B., Stephansson, O., 1997. Rock stress and its measurement. Chapman and Hall, London, p.
371 490.
- 372 Amato, A., Selvaggi, G., 1993. Aftershock location and P-velocity structure in the epicentral region
373 of the 1980 Irpinia earthquake. *Ann. Geofis.* 36, 3-15.
- 374 Amato, A., Montone, P., Cesaro, M., 1995. State of stress in southern Italy from borehole breakout
375 and focal mechanisms data. *Geophys. Res. Lett.* 22, 3119-3122.
- 376 Ascione, A., Cinque, A., Improta, L., Villani, F., 2003. Late Quaternary faulting within the Southern
377 Apennines seismic belt: new data from Mt. Marzano area (Southern Italy). *Quaternary International*
378 101-102, 27-41.
- 379 Azzara, R., Basili, A., Beranzoli, L., Chiarabba, C., Di Giovambattista, R., Selvaggi, G., 1993. The
380 seismic sequence of Potenza (May 1990). *Ann. Geofis.* 36 (1), 237-243.
- 381 Babcock, E.A., 1978. Measurement of subsurface fractures from dipmeter logs. *AAPG Bulletin* 62
382 (7), 1111-1126. Reprinted in 1990, in Foster, N.H., and Beaumont, E.A., eds., *Formation evaluation*
383 *II-log-interpretation: AAPG Treatise of Petroleum Geology Reprint Series n. 17*, pp. 457-472.

- 384 Barton, C.A., Zoback, M.D., 1994. Stress perturbations associated with active stress faults
385 penetrated by boreholes: Possible evidence for near-complete stress drop and the a new technique for
386 stress magnitude measurements. *J. Geophys. Res.* 99 (B5), 9373-9390.
- 387 Bell, J.S., Gough, D.I., 1979. Northeast-southwest compressive stress in Alberta: evidence from oil
388 wells. *Earth and Plan. Sc. Lett.* 45, 475-482.
- 389 Bell, J.S., Gough, D.I., 1983. The use of borehole breakout in the study of crustal stress, in
390 Hydraulic fracturing stress measurements. Edit by D.C., National Academy press, Washington.
- 391 Bell, J.S., Caillet, G., Adams, J., 1992. Attempts to detect open fractures and non-sealing faults with
392 dipmeter logs. *Geological Society, London, Special Publications* 65, 211-220,
393 doi:10.1144/GSL.SP.1992.065.01.16.
- 394 Bernard, P., Zollo, A., 1989. The Irpinia (Italy) 1980 Earthquake: Detailed Analysis of a Complex
395 Normal Faulting. *J. Geophys. Res.* 94, 1631-1648.
- 396 Bonardi, G., D'Argenio, B., Perrone, V., 1988. Carta geologica dell'Appennino meridionale alla
397 scala 1:250.000. *Mem. Soc. Geol. It.* 41, 1341, 1 tav.
- 398 Boschi, E., Mulargia, F., Mantovani, E., Bonafede, M., Dziewonski, A.M., Woodhouse, J.H., 1981.
399 The Irpinia earthquake of Novembre 23, 1980. *Eos Trans. AGU* 6, p. 330.
- 400 Boschi, E., Pantosti, D., Slejko, D., Stucchi, M., Valensise, G., 1993. Special issue on the meeting
401 "Irpinia Dieci anni i Dopo", Sorrento 19-24 November 1990. *Ann. Geofis.* 36 (1), 353 pp,
402 Editrice Compositori.
- 403 Butler, R.W.H., Mazzoli, S., Corrado, S., De Donatis, S., Di Bucci, D., Gambini, R., Naso, G.,
404 Nicolai, C., Scrocca, D., Shiner, P., Zucconi, V., 2004. Applying thick-skinned tectonic models to
405 the Apennine thrust belt of Italy—Limitations and implications, in: K. R. McClay (Ed.), *Thrust*
406 *tectonics and hydrocarbon systems. AAPG Memoir* 82, 647–667.
- 407 Caiazza, C., Giovine, G., Ortolani, F., Pagliuca, S., Schiattarella, M., Vitale, C., 1992. Genesi ed
408 evoluzione strutturale della depressione tettonica dell'Alta Valle del Sele (Appennino Campano-
409 Lucano). *Studi Geologici Camerti* 1, 245–255.
- 410 Casero, P., Roure, F., Endignoux, L., Moretti, C., Sage, L., Vially, R., 1988. Neogene geodynamic
411 evolution of the Southern Apennines. *Mem. Soc. Geol. It.* 41 (1), 109-120.
- 412 Casero, P., Roure, F., Vially R., 1991. Tectonic framework and petroleum potential of the southern
413 Apennines, In *Generation, accumulation and production of Europe's hydrocarbons*, edited by
414 Spencer A.M., *Spec. Publ. European Assoc. Petroleum Geosci.* 1, 381-387.
- 415 Castello, B., Moschillo, R., Pignone, M., Vinci, S., Doumaz, F., Nostro, C., Selvaggi, G., 2008.
416 Carta della sismicità in Italia 2000-2007. <http://csi.rm.ingv.it/>, 2008.

- 417 Castillo, D.A., Zoback, M.D., 1994. Systematic variations in stress state in the southern San Joaquin
418 Valley: inferences based on well-bore data and contemporary seismicity. *Am. Ass. Petrol. Geol.*
419 *Bull.* 78 (8), 1257-1275.
- 420 Cello, G., Paltrinieri, W., Tortrici, L., 1987. Caratterizzazione strutturale delle zone esterne
421 dell'Appennino molisano. *Mem. Soc. Geol. It.* 38, 155-161.
- 422 Cello, G., Martini, N., Paltrinieri, W., Tortorici, L., 1989. Structural styles in the frontal zones of the
423 Southern Apennines, Italy: an example from the Molise district. *Tectonics* 8, 753–768.
- 424 Chiarabba, C., Amato, A., 1994. From tomographic images to fault heterogeneities. *Ann. Geofis.* 37
425 (6), 1481-1494.
- 426 Cinque, A., Patacca, E., Scandone, P., Tozzi, M., 1993. Quaternary kinematic evolution of the
427 Southern Apennines. Relationships between surface geological features and deep lithospheric
428 structures. *Ann. Geofis.* 36 (2), 249-260.
- 429 Cinti, F.R., Faenza, L., Marzocchi, W., Montone, P., 2004. Probability map of the next $M \geq 5.5$
430 earthquakes in Italy. *Geochem. Geophys. and Geosystems* 5 (11), doi:10.1029/2004GC000724.
- 431 Cippitelli, G., 2007. The Crop-04 seismic profile. Interpretation and structural setting of the
432 Agropoli-Barletta Geotraverse, in: Mazzotti, A., Patacca, E., Scandone, P. (Eds), Results of the
433 CROP Project sub-project CROP04 southern Apennines (Italy), *Boll. Soc. Geol. It.*, special issue 7,
434 267-281.
- 435 Cocco, M., Chiarabba, C., Di Bona, M., Selvaggi, G., Margheriti, L., Frepoli, A., Lucente, F.P.,
436 Basili, A., Jongmans, D., Campillo, M., 1999. The April 1996 Irpinia seismic sequence: evidence for
437 fault interaction. *J. of Seism.* 3, 105-117.
- 438 CPTI Working Group, Catalogo parametrico dei terremoti Italiani, version 2004 (CPTI04), Istituto
439 Nazionale di Geofisica e Vulcanologia, Bologna, 2004. (Available at
440 <http://emidius.mi.ingv.it/CPTI>).
- 441 Cucci, L., Pondrelli, S., Frepoli, A., Mariucci, M.T., Moro, M., 2004. A multidisciplinary approach
442 for the characterization of the seismogenic sources in seismic gap areas: first results from the
443 Pergola-Melandro basin and the Agri valley (Southern Italy). *Geophys. J. Int.* 156, 575-583,
444 doi:10.1111/j.1365-246X.2004.02161.x.
- 445 D'Argenio, B., Pescatore, T., Scandone, P., 1973. Schema geologico dell'Appennino meridionale
446 (Campania e Lucania). *Atti Acc. Naz. Lincei, Quad.* 183, 49-73.
- 447 Deschamps, A., King, G.C.P., 1980. The Campania Lucania (southern Italy) earthquake of
448 November 23, 1980. *Earth Planet. Sci. Lett.* 62, 296-304.
- 449 Deschamps, A., King, G.C.P., 1984. Aftershocks of the Campania-Lucania (Italy) earthquake of 23
450 November 1980. *Bull. Seismol. Soc. Am.* 74, 2483-2517.

- 451 Dewey, J.F., Helman, M.L., Turco, E., Hutton, D.H.W., Knott, S.D., 1989. Kinematics of the
452 western Mediterranean, in: Coward, M.P., Dietrich, D., Park, R.G. (Eds.), *Alpine Tectonics*,
453 Geological Society Special Publication 45, 265-283.
- 454 Di Luccio, F., Piscini, A., Pino, N.A., Ventura, G., 2005. Reactivation of deep faults beneath
455 southern Apennines: evidence from the 1990-1991 Potenza seismic sequences. *Terra Nova* 17, 586-
456 590.
- 457 Ding, Y.C., Zhang, D.L., 1991. Application of rock acoustic emission in crustal stress measurement.
458 *J. of Rock Mechanics and Engineering* 10 (4), 326-331.
- 459 Doglioni, C., 1991. A proposal of kinematic modelling for W-dipping subductions - possible
460 applications to the Tyrrhenian-Apennines system. *Terra Nova* 3, 423-434.
- 461 Doglioni, C., Harabaglia, P., Martinelli, G., Mongelli, F., Zito, G., 1996. A geodynamic model of the
462 Southern Apennines accretionary wedge. *Terra Nova* 8, 540-547.
- 463 Ekström, G., 1994. Teleseismic analysis of the 1990 and 1991 earthquakes near Potenza. *Ann.*
464 *Geofis.* 37, 1591-1599.
- 465 Esposito, E., Luongo, G., Maturano, A., Porfido, S., 1988. I terremoti recenti dal 1980 al 1986
466 nell'Appennino meridionale. *Mem. Soc. Geol. It.* 41 (2), 1117-1128.
- 467 Faenza, L., Pierdominici, S., 2007. Statistical occurrence analysis and spatio-temporal distribution
468 of earthquakes in the Apennines (Italy). *Tectonophysics* 439, 13-31,
469 doi:10.1016/j.tecto.2007.02.019.
- 470 Frepoli, A., Amato, A., 2000. Fault-plane solutions of crustal earthquakes in southern Italy (1988-
471 1995): seismotectonic implications. *Ann. Geofis.* 43, 437-467.
- 472 Frepoli, A., Cinti, F.R., Amicucci, L., Cimini, G.B., De Gori, P., Pierdominici, S., 2005. Pattern of
473 seismicity in the Lucanian Apennines and foredeep (Southern Italy) from recording by SAPTEX
474 temporary array. *Ann. Geophys* 48 (6), 1035-1054.
- 475 Galadini, F., Meletti, C., Vittori, E.A., 2000. Stato delle conoscenze sulle faglie attive in Italia:
476 elementi geologici di superficie: Risultati del Progetto 5.1.2 "Inventario delle faglie attive e dei
477 terremoti ad esse associabili, in *Le ricerche del GNDT nel campo della pericolosità sismica (1996-
478 1999)*, in: Galadini, F., Meletti, C., Rebez, A. (Eds), pp. 107-136, CNR- Gruppo Nazionale per la
479 Difesa dai Terremoti, Roma.
- 480 Gasparini, P., Iannaccone, G., Scarpa, R., 1985. Fault-plane solutions and seismicity of the Italian
481 peninsula. *Tectonophysics* 117, 59-78.
- 482 Giano, S., Maschio, L., Alessio, M., Ferranti, L., Improta, L., Schiattarella, M., 2000. Radiocarbon
483 dating of active faulting in the High Agri Valley, southern Italy. *J. of Geodyn.* 29, 371-386.

- 484 Giardini, D., 1993. Teleseismic observation of the November 23 1980, Irpinia earthquake. *Ann.*
485 *Geofis.* 36 (1), 17-25.
- 486 Haimson, B.C., Heirrick, C.G., 1986. Borehole breakouts- a new tool for estimating in situ stress? in:
487 O. Stephansson (Ed), *Proceedings International Symposium on Rock Stress and Rock Stress*
488 *Measurements*, pp. 271-280, Stockholm.
- 489 Heidbach, O., Tingay, M., Barth, A., Reinecker, J., Kurfeß, D., Müller, B., 2008. The 2008 release
490 of the World Stress Map. (available online at www.world-stress-map.org)
- 491 Improta, L., Bonagura, M., Capuano, P., Iannaccone, G., 2003. An integrated geophysical
492 investigation of the upper crust in the epicentral area of the 1980, Ms=6.9, Irpinia earthquake
493 (Southern Italy). *Tectonophysics* 361, 139-169.
- 494 INGV-CNT Seismic Bulletin <http://csi.rm.ingv.it>
- 495 Lavecchia, G., 1988. The Tyrrhenian Apennines system: structural setting and seismotectogenesis.
496 *Tectonophysics* 147, 263-296.
- 497 Lentini, F., Carbone, S., Di Stefano, A., Guarnieri, P., 2002. Stratigraphical and structural constraints
498 in the Lucanian Apennines (southern Italy): tools for reconstructing the geological evolution. *J. of*
499 *Geodyn.* 34 (1), 141-158.
- 500 Maggi, C., Frepoli, A., Cimini, G.B., Console, R., Chiappini, M., 2009. Recent seismicity and
501 crustal stress field in the Lucanian Apennines and surrounding areas (Southern Italy): seismotectonic
502 implications. *Tectonophysics* 463, 130–144.
- 503 Malinverno, A., Ryan, W.B.F., 1986. Extension in the Tyrrhenian Sea and shortening in the
504 Apennines as a result of arc migration driven by sinking of the lithosphere. *Tectonics* 5, 227–245.
- 505 Mardia, K.V., 1972. *Statistics of directional data*, Academic Press, San Diego, California, pp. 357.
- 506 Mariucci, M.T., Amato, A., Gambini, R., Giorgioni, M., Montone, P., 2002. Along-depth stress
507 rotations and active faults: An example in a 5-km deep well of southern Italy. *Tectonics* 21 (4),
508 1021, 10.1029/2001TC001338.
- 509 Marturano, A., Esposito, E., Porfido, S., Luongo, G., 1988. Il terremoto del 4 ottobre 1983
510 (Pozzuoli); attenuazione dell'intensita con la distanza e relazione magnitudino-intensita; zonazione
511 della Città di Napoli. *Mem. Soc. Geol. It.* 41 (2), 941-948.
- 512 Marzocchi, W., Selva, J., Cinti, F.R., Montone, P., Pierdominici, S., Schivardi, R., Boschi, E., 2009.
513 On the occurrence of large earthquakes: New insights from a model based on interacting faults
514 embedded in a realistic tectonic setting. *J. of Geophys. Res.* 114 (B01307),
515 doi:10.1029/2008JB005822.

- 516 Mazzoli, S., Helman, M., 1994. Neogene patterns of relative plate motion for Africa-Europe: some
517 implications for recent central Mediterranean tectonics. *Geologische Rundschau* 83, 464-468.
- 518 Mazzoli, S., Invernizzi, C., Marchegiani, L., Mattioni, L., Cello, G., 2004. Brittle-ductile shear zone
519 evolution and fault initiation in limestones, Monte Cugnone (Lucania), southern Apennines, Italy,
520 in: Alsop, I., Holdsworth, R.E. (Eds.), *Transport and Flow Processes in Shear Zones*, Geological
521 Society, London, Special Publications 224, 353-373.
- 522 Michetti, A.M., Ferrelli, L., Esposito, E., Porfido, E., Blumetti, A.M., Vittori, E., Serva, L., Roberts
523 G.P., 2000. Ground effects during the 9 september 1998, Mw=5.6, Lauria earthquake and the
524 seismic potential of the “aseismic” Pollino region in Southern Italy. *Seism. Res. Let.* 41 (1), 31-46.
- 525 Montone, P., Amato, A., Frepoli, A., Mariucci, M.T., Cesaro, M., 1997. Crustal stress regime in
526 Italy. *Ann. Geofis.* 40 (3), 741-757.
- 527 Montone, P., Mariucci, M.T., Pondrelli, S., Amato, A., 2004. An improved stress map for Italy and
528 surrounding regions (central Mediterranean). *J. Geophys. Res.* 109(B10410),
529 doi:10.1029/2003JB002703.
- 530 Mostardini, F., Merlini, S., 1986. Appennino centro-meridionale. Sezioni geologiche e proposta di
531 modello strutturale. *Mem. Soc. Geol. It.* 35, 177-202.
- 532 Pantosti, D., Valensise, G., 1990. Faulting mechanism and complexity of the 23 November, 1980,
533 Campania-Lucania earthquake inferred from surface observations. *J. Geophys. Res.* 95 (B10),
534 15319-15341.
- 535 Pantosti, D., Valensise, G., 1993. Source geometry and long-term behavior of the 1980, Irpinia
536 earthquake fault based on field geologic observations. *Ann. Geofis.* 36 (1), 41-49.
- 537 Pantosti, D., Schwartz, D.P., Valensise, G., 1993. Paleoseismology along the 1980 surface rupture of
538 the Irpinia fault: implications for earthquake recurrence in the southern Apennines, Italy. *J. Geophys.*
539 *Res.* 98 (B4), 6561-6577.
- 540 Patacca, E., 2007. Stratigraphic constraints on the CROP-04 seismic line interpretation, in: Mazzotti,
541 A., Patacca, E., Scandone, P. (Eds), *Results of the CROP Project sub-project CROP04 southern*
542 *Apennines (Italy)*, *Boll. Soc. Geol. It.*, special issue, 7, 185-239.
- 543 Patacca, E., Scandone, P., 1989. Post-Tortonian mountain building in the Apennines: The role of the
544 passive sinking of a relic lithosphere slab, in Boriani, A. et al. (Eds), *The lithosphere in Italy*,
545 *Advances in Earth Science Research* 80, , pp. 157-176, Acc. Naz. dei Lincei, Rome.
- 546 Patacca, E., Scandone, P., 2001. Late thrust propagation and sedimentary response in the thrust-belt-
547 foredeep system of the southern Apennines (Pliocene-Pleistocene), in: Vai, G.B., Martini, I.P. (Eds),
548 *Anatomy of an Orogen: the Apennines and adjacent Mediterranean Basins*, pp. 401-440, Kluwer
549 Academic Publishers.

- 550 Patacca, E., Scandone, P., 2004. The Plio-Pleistocene thrust belt-foredeep system in the southern
551 Apennines and Sicily (Southern Apenninic Arc, Italy), in: Crescenti, U., D'offizi, S., Merlini, S.,
552 Sacchi, R. (Eds), *Geology of Italy, spec. vol. Ital. Geol. Soc. IGC 32 Florence 2004*, 93-129.
- 553 Patacca, E., Scandone, P., 2007. Constraints on interpretation of the CROP-04 seismic line derived
554 from Plio-Pleistocene foredeep and thrust-sheet-top deposits, in: Mazzotti, A., Patacca, E.,
555 Scandone, P. (Eds), *Results of the CROP Project sub-project CROP04 southern Apennines (Italy)*,
556 *Boll. Soc. Geol. It., special issue 7*, 241-256.
- 557 Patacca, E., Scandone, P., Sartori, R., 1990. Tyrrhenian basin and Apenninic arcs: kinematic
558 relations since Late Tortonian times. *Mem. Soc. Geol. It.* 45, 425-451.
- 559 Pescatore, T., Renda, P., Schiattarella, M., Tramutoli, M., 1999. Stratigraphic and structural
560 relationships between Meso-Cenozoic Lagonegro basin and coeval carbonate platforms in Southern
561 Apennines, Italy. *Tectonophysics* 315 (1-4), 269-286.
- 562 Pieri, P., Vitale, G., Beneduce, P., Doglioni, C., Gallicchio, S., Giano, S.I., Loizzo, R., Moretti, M.,
563 Prosser, G., Sabato, L., Schiattarella, M., Tramutoli M., Tropeano, M., 1997. Tettonica quaternaria
564 nell'area bradanico-ionica. *Il Quaternario* 10, 535-542.
- 565 Plumb, R.A., Hickman, S.H., 1985. Stress-induced borehole elongation: a comparison between the
566 four-arm dipmeter and the borehole televiewer in the Auburn geothermal well. *J. Geophys. Res.* 90
567 (B7), 5513-5521.
- 568 Plumb, R.A., Cox, J.W., 1987. Stress directions in eastern North America determined to 4.5 km from
569 borehole elongation measurements. *J. Geophys. Res.* 92, 4805-4816.
- 570 Pondrelli, S., Morelli, A., Ekström, G., Mazza, S., Boschi, E., Dziewonski, A.M., 2002. European-
571 Mediterranean regional centroid-moment tensors; 1997-2000. *Phys. Earth Planet. Int.* 130 (1-2), 71-
572 101.
- 573 Pondrelli, S., Salimbeni, S., Ekström, G., Morelli, A., Gasperini, P., Vannucci G., 2006. The Italian
574 CMT dataset from 1977 to the present. *Phys. Earth Planet. Int.* 159 (3-4), 286-303,
575 doi:10.1016/j.pepi.2006.07.008, available at www.ingv.it/seismoglo/RCMT.
- 576 Porfido, S., Esposito, E., Luongo, G., Maturano, A., 1988. I terremoti del XIX secolo dell'Appennino
577 Campano-Lucano. *Mem. Soc. Geol. It.* 41 (2), 1105-1116.
- 578 Roure, F., Casero, P., Vially, R., 1991. Growth processes and melange formation in the southern
579 Apennines accretionary wedge. *Earth Plan. Sci. Lett.* 102, 395-412.
- 580 Scandone, P., Mazzotti, A., Fradelizio, G.L., Patacca, E., Stucchi, E., Tozzi, M., Zanzi, L., 2003.
581 Line CROP 04: Southern Apennines, in: Scrocca, D., Doglioni, C., Innocenti, F., Manetti, P.,
582 Mazzotti, A., Bertelli, L., Burbi, L., D'Offizi, S. (Eds), *Crop Atlas – Seismic reflection profiles of*
583 *the Italian crust*, *Mem. Desc. della Carta Geol. d'It.* 62, 155-165.

- 584 Schiattarella, M., Di Leo, P., Beneduce, P., Giano, I.S., 2003. Quaternary uplift vs tectonic loading:
585 a case study from the Lucanian Apennine, southern Italy. *Quaternary Int.* 101-102, 239-251.
- 586 Scrocca, D., Sciamanna, S., Di Luzio, E., Tozzi, M., Nicolai, C., Gambini, R., 2007. Structural
587 setting along the CROP-04 deep seismic profile (Southern Apennines – Italy), in: Mazzotti, A.,
588 Patacca, E., Scandone, P. (Eds), *Results of the CROP Project sub-project CROP04 southern*
589 *Apennines (Italy)*, *Boll. Soc. Geol. It.*, special issue, 7, 283-296.
- 590 Seto, M., Utagawa, M., Katsuyama, K., Kiyama, T., 1998. In situ stress determination using AE and
591 DRA techniques. *Int. J. Rock Mech. and Min. Sci. & Geomech. Abs.* 35 (4-5), 458-459.
- 592 Shamir, G., Zoback, M.D., 1992. Stress orientation profile to 3.5km depth near the San Andreas
593 Fault at Cajon Pass, California. *J. Geophys. Res.* 97 (B4), 5059-5080.
- 594 Valensise, G., Pantosti, D., 2001. The investigation of potential earthquake sources in peninsular
595 Italy: a review. *J. of Seismol.* 5, 287-306.
- 596 Westaway, R., Jackson, J., 1984. Surface faulting in the southern Italian Campania-Basilicata
597 earthquake of 23 November 1980. *Nature* 312, 436-438.
- 598 Westaway, R., Jackson, J., 1987. The earthquake of 1980 November 23 in Campania-Basilicata
599 (southern Italy). *Geophys. J. R. Astr. Soc.* 90, 375-443.
- 600 Wu, H.Y., Ma, K.F., Zoback, M.D., Boness, N., Ito, H., Hung, J.H., Hickman, S., 2007. Stress
601 orientations of Taiwan Chelungpu-Fault Drilling Project (TCDP) hole-A as observed from
602 geophysical logs. *Geophys. Res. Lett.* 34, L01303, doi:10.1029/2006GL028050.
- 603 Wu, Y.H., Yeh, E.C., Dong, J.J., Kuo, L.W., Hsu, J.Y., Hung, J.H., 2008. Core-log integration
604 studies in hole-A of Taiwan Chelungpu-fault Drilling Project. *Geophys. J. Int.* 174, 949-965.
- 605 Zheng, Z., Kemeny, J., Cook, N.G., 1989. Analysis of borehole breakout. *J. Geophys. Res.* 94, 7171-
606 7182.
- 607 Zoback, M.L., 1992. First- and second-order patterns of stress in the lithosphere: the world stress
608 map project. *J. Geophys. Res.* 97 (B8), 703-728.
- 609 Zoback, M.L., Zoback, M.D., 1980. State of stress in the conterminous United States. *J. Geophys.*
610 *Res.* 85 (B11), 6113-6156.
- 611 Zoback, M.D., Zoback, M.L., 1991. Tectonic stress field of North America and relative plate
612 motions, in: Slemmons, D.B., Engdahl, E.R., Zoback, M.D., Blackwell, D.D., *The Geology of North*
613 *America. Neotectonics of North America*, *Geol. Soc. Am.* 339-366.
- 614 Zoback, M.D., Moos, D., Mastin, L., Anderson, R.N., 1985. Well bore breakouts and in situ stress. *J.*
615 *Geophys. Res.* 90 (B7), 5523-5530.

616 Zoback, M.L., Zoback, M.D., Adams, J., Assumpção, M., Bell, S., Bergman, E.A., Blumling, P.,
 617 Brereton, N.R., Denham, D., Ding, J., Fuchs, K., Gay, N., Gregersen, S., Gupta, H.K., Gvishiani, A.,
 618 Jacob, K., Klein, R., Knoll, P., Magee, M., Mercier, J.L., Müller, B.C., Paquin, C., Rajendran, K.,
 619 Stephansson, O., Suarez, G., Suter, M., Udias, A., Xu, Z.H., Zhizhin, M., 1989. Global patterns of
 620 tectonic stress. *Nature* 341, 291-298.

621 **Figure Captions**

622 **Figure 1.** Above: schematic structural map (modified after Scrocca et al., 2007): 1. Main out of
 623 sequence thrust; 2. Buried Apenninic thrust front; 3. CROP-04 seismic line; 4. Wells. Below: part of
 624 CROP-04 cross-section (section A-A'; modified after Cippitelli, 2007 according to the stratigraphic
 625 description of Patacca, 2007 from c. to e. deposits). Legend: a. Castelgrande Sandstone (Miocene);
 626 b. Cilento Flysch and Liguride-Sicilide complex (Cretaceous-Paleogene); c. Apenninic carbonate
 627 Platform (Alburno-Cervati; late Triassic); d. Lagonegro II unit (early Triassic-early Cretaceous) e.
 628 Apulian carbonate Platform (Dogger-early Pliocene); f. Permo-Triassic substratum; g. Normal fault;
 629 h. Reverse fault-overthrust plane; i. Unconformity.

630
 631 **Figure 2.** Regional overview of present-day stress data and seismicity. The black arrows indicate the
 632 S_{hmin} average orientation obtained by all the stress indicators. Historical seismicity from 217 B.C. to
 633 1980 ($M \geq 5.5$; CPTI Working Group, 2004); instrumental seismicity from 1981 to present (INGV-
 634 CNT Seismic Bulletin <http://csi.rm.ingv.it>); fault plane solutions of the largest earthquakes (see
 635 Table 1 for references).

636
 637 **Figure 3.** a) Map of the Irpinia Fault System and its segments breaking at 0s, 20s and 40s with the
 638 associated focal mechanism solutions. The stars represent the earthquake epicenters (modified from
 639 Pantosti and Valensise, 1990); b) zoom of the Marzano-Carpineta fault segment with the location of
 640 the San Gregorio Magno 1 well.

641
 642 **Figure 4.** Breakout data along the San Gregorio Magno 1 well: a) synthetic stratigraphic log of the
 643 main lithological and tectonic units (Patacca, 2007); b) available data interval; c) breakout zones: the
 644 size of the black rectangle represents the length of the breakout data with the same direction; d)
 645 individual breakout azimuths; e) clockwise and anticlockwise breakout rotations with respect to the
 646 regional trend; f) and g) rose diagrams of breakout results for lithological and tectonic unit; h) total
 647 rose diagram. The light grey box represents the interval in which the borehole should intersect the
 648 Irpinia fault hypothesizing different fault dips (from 60° to 75°). Legend of a): 1. stratigraphic
 649 discontinuity; 2. normal fault; 3. thrust fault.

650
 651 **Figure 5.** Geological and geophysical data of the San Gregorio Magno 1 well. a) Synthetic
 652 stratigraphic log of the main lithological and tectonic units (Patacca, 2007); b) washout zones; c)
 653 downhole logs; d) breakout azimuths; e) five boxes showing the magnification of the five selected
 654 sectors (in red the anomalous trend). The light grey boxes indicate possible shear zones (A, B, C, D
 655 and E sectors). See text for the explanation of zone 1, 2, 3 and 4.

656
 657 **Figure 6.** Present-day stress data in southern Apennines. Breakouts are relative to SGM1 and wells
 658 from Montone et al., 2004. Focal mechanisms of main earthquakes and seismic sequences are shown
 659 (the numbers refer to Table 1, see References therein). Colours correspond to different types of focal
 660 solutions: brown, normal faulting with NE-SW extension; yellow, strike-slip faulting; orange,
 661 normal faulting with strike slip component and NE-SW to E-W extension; pink, normal faulting
 662 with strike slip component and N-S to NNE-SSW extension; violet, normal faulting with strike slip
 663 component and NW-SE extension.

664
665
666
667
668
669
670
671
672
673
674
675
676

Figure 7. - The cross-section (modified from Cippitelli, 2007) shows the three hypotheses of the Irpinia fault trend. If the SGM1 well crosses the Irpinia fault at 2350m: i) a straight fault plane 60° dipping from surface to focal depth (red fault); ii) a fault plane changing dip from 70° at surface to 60° in the upper kilometer (blue fault). If the SGM1 well crosses the Irpinia fault at 3800m: iii) a 70° dipping fault changing to 60° down to focal depth (yellow fault). The red star represents the mainshock at 0s and the grey area around it indicates the associated error in vertical and horizontal location of about 3km and 1km respectively (Bernard and Zollo, 1989). Legend: a. Castelgrande Sandstone (Miocene); b. Cilento Flysch and Liguride-Sicilide complex (Cretaceous-Paleogene); c. Apenninic carbonate Platform (Alburno-Cervati; late Triassic); d. Lagonegro II unit; (early Triassic-early Cretaceous) e. Apulian carbonate Platform (Dogger-early Pliocene); f. Permo-Triassic substratum; g. Normal fault; h. Reverse fault-overthrust plane; i. Unconformity.

676 Research highlights

677

678

- Horizontal stress orientations in the well are consistent with the regional trend.

679

- Anomalous stress orientations reveal local stress sources

680

- faults cause log anomalies in a well

681

- fault-well intersection at depth can be defined

682

- downhole logs help in defining fault geometry at depth

683

Accepted Manuscript

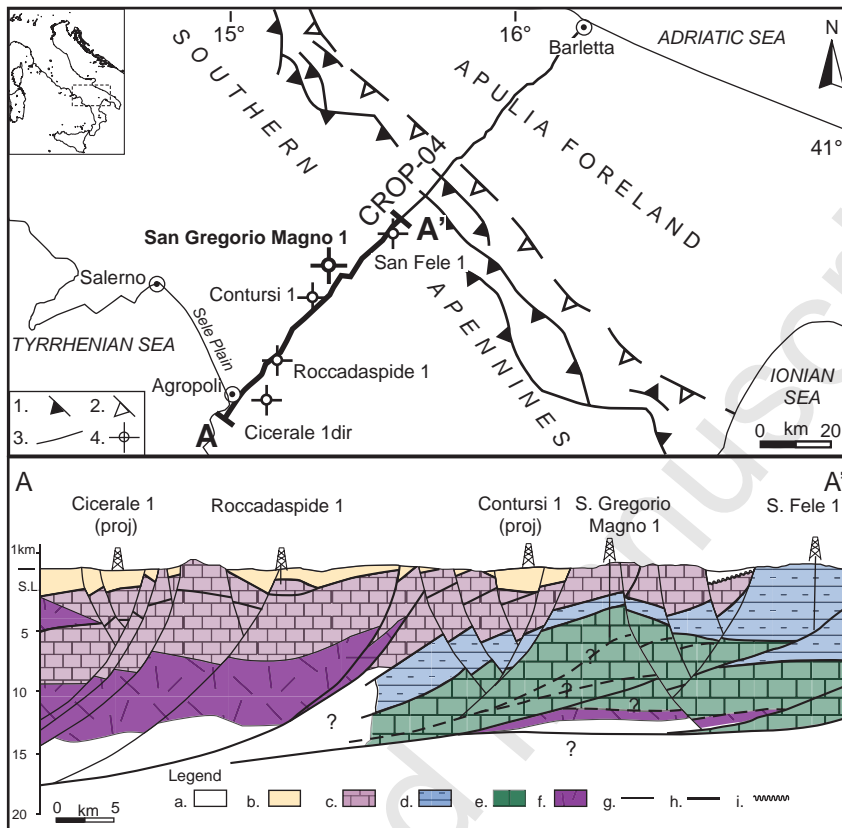


Figure 1

Figure 2

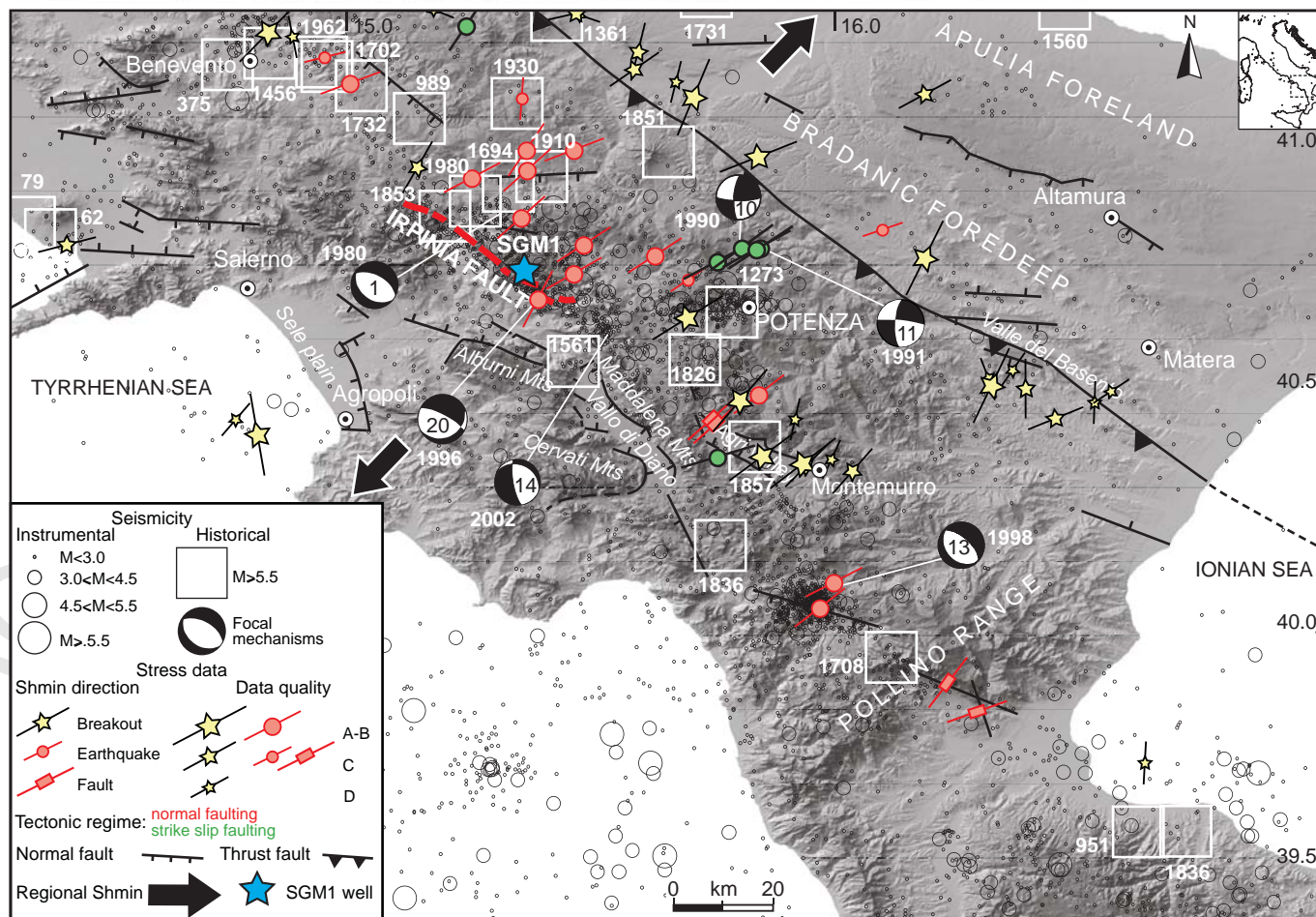


Figure 2

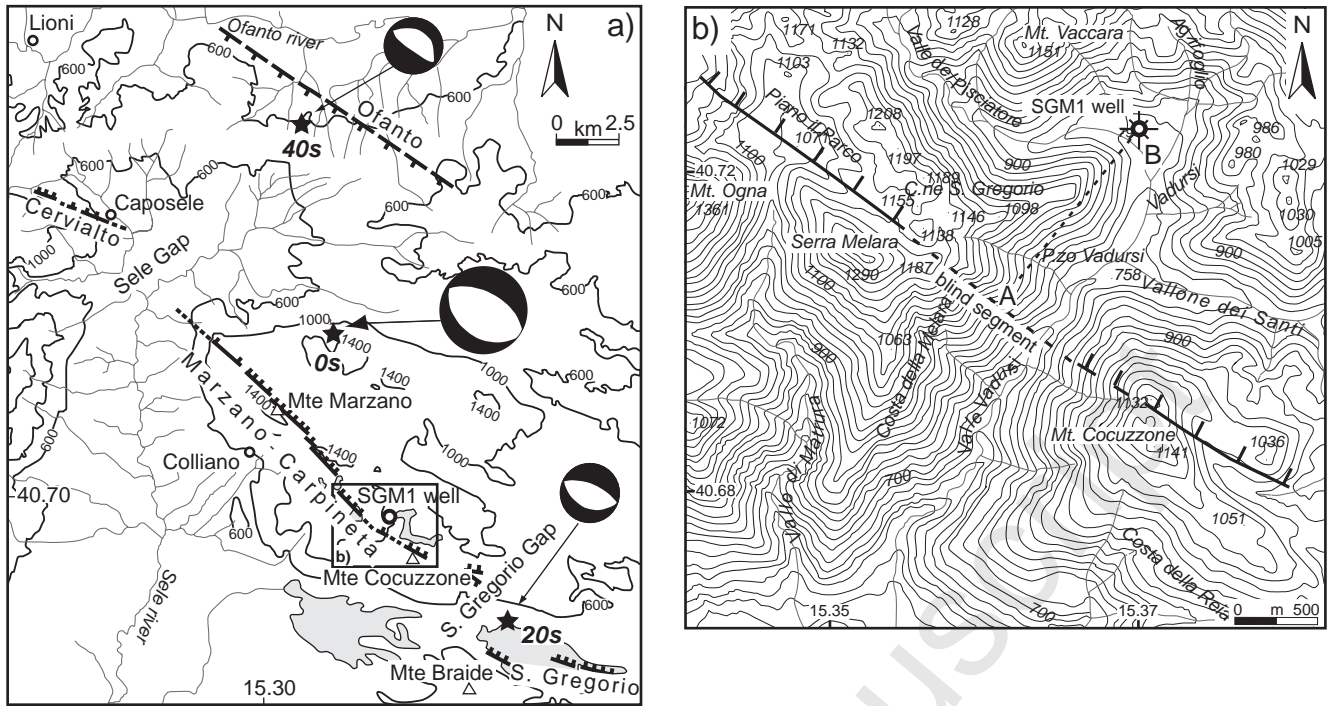


Figure 3

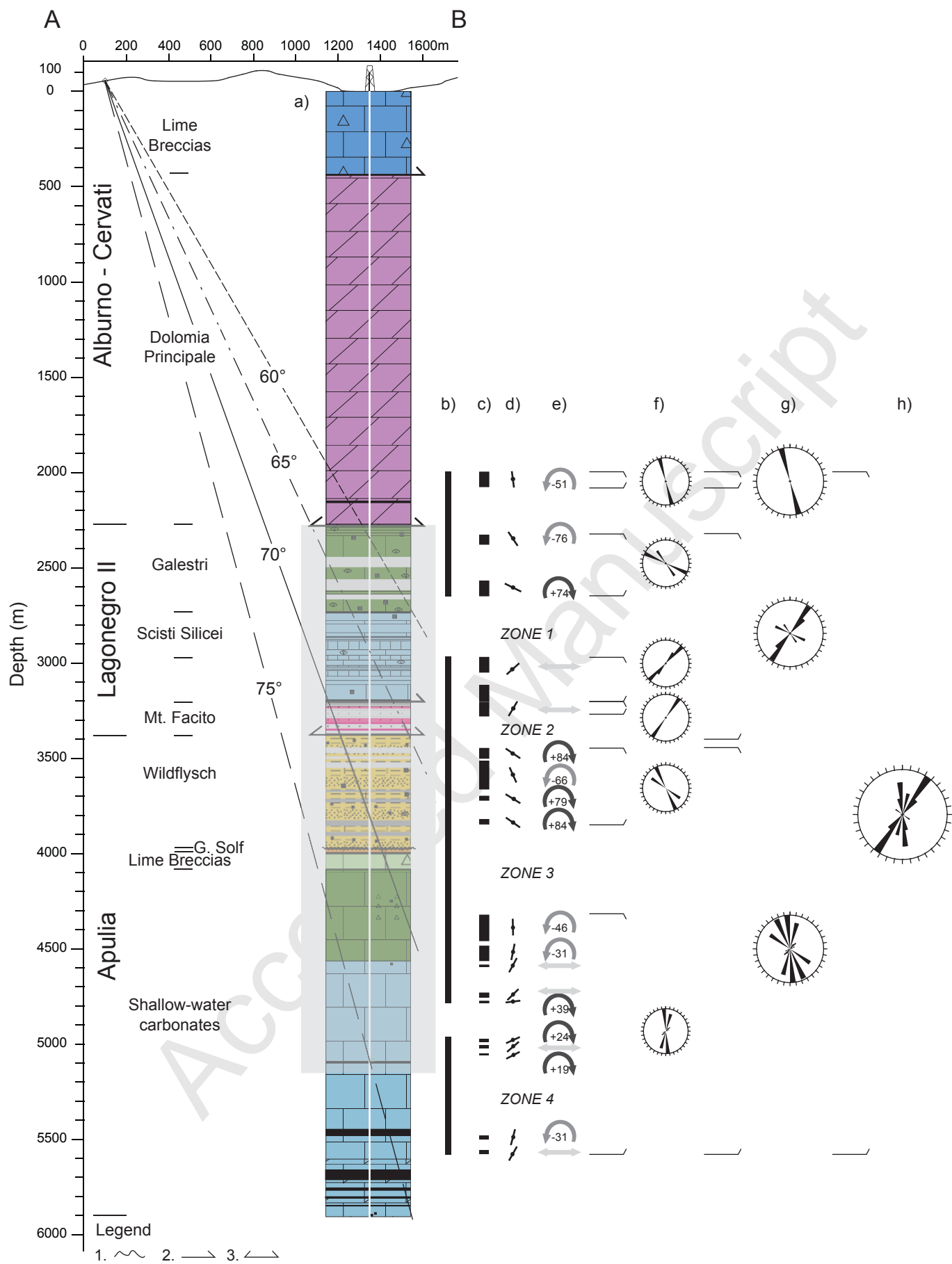


Figure 4

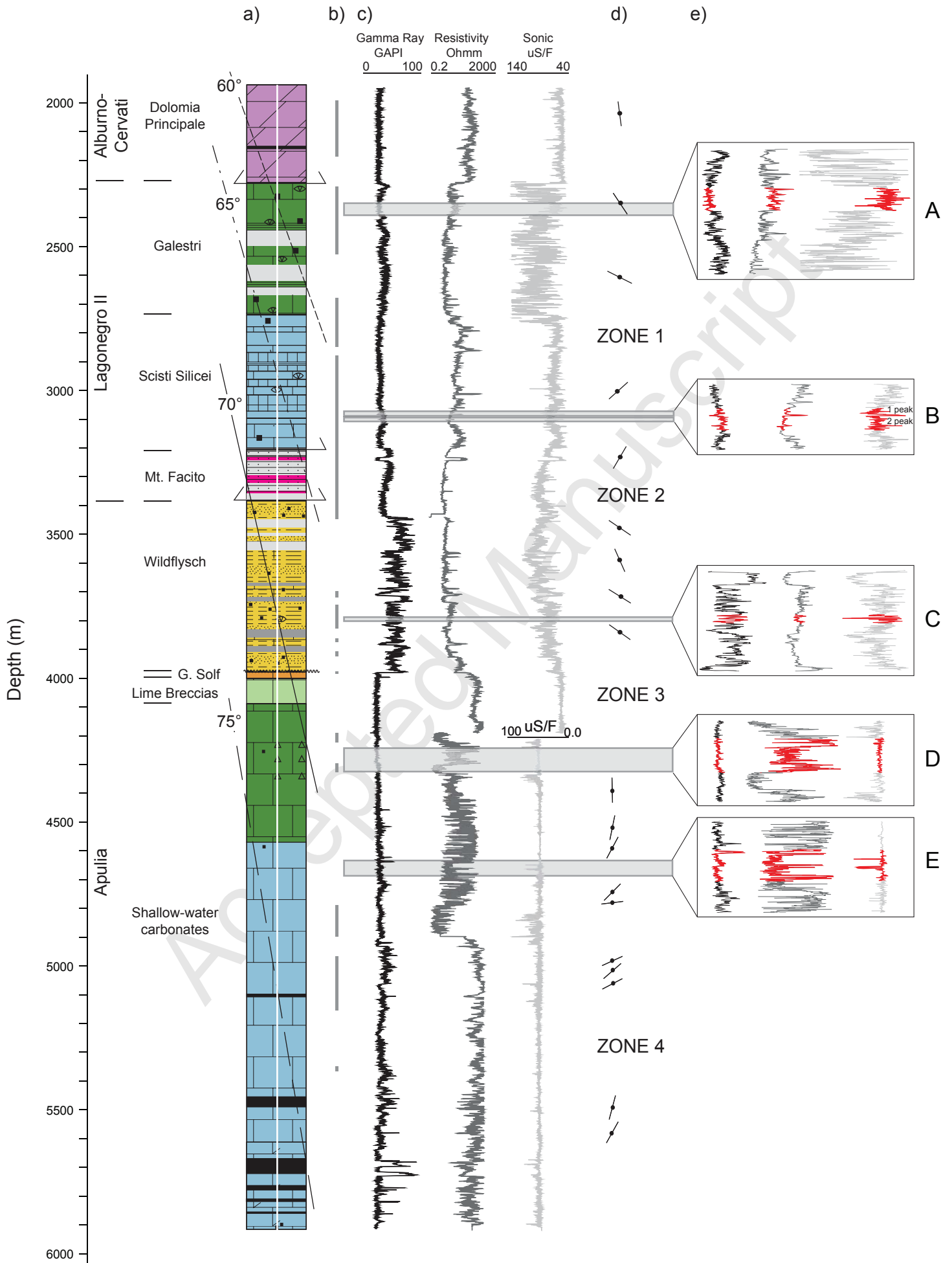


Figure 5

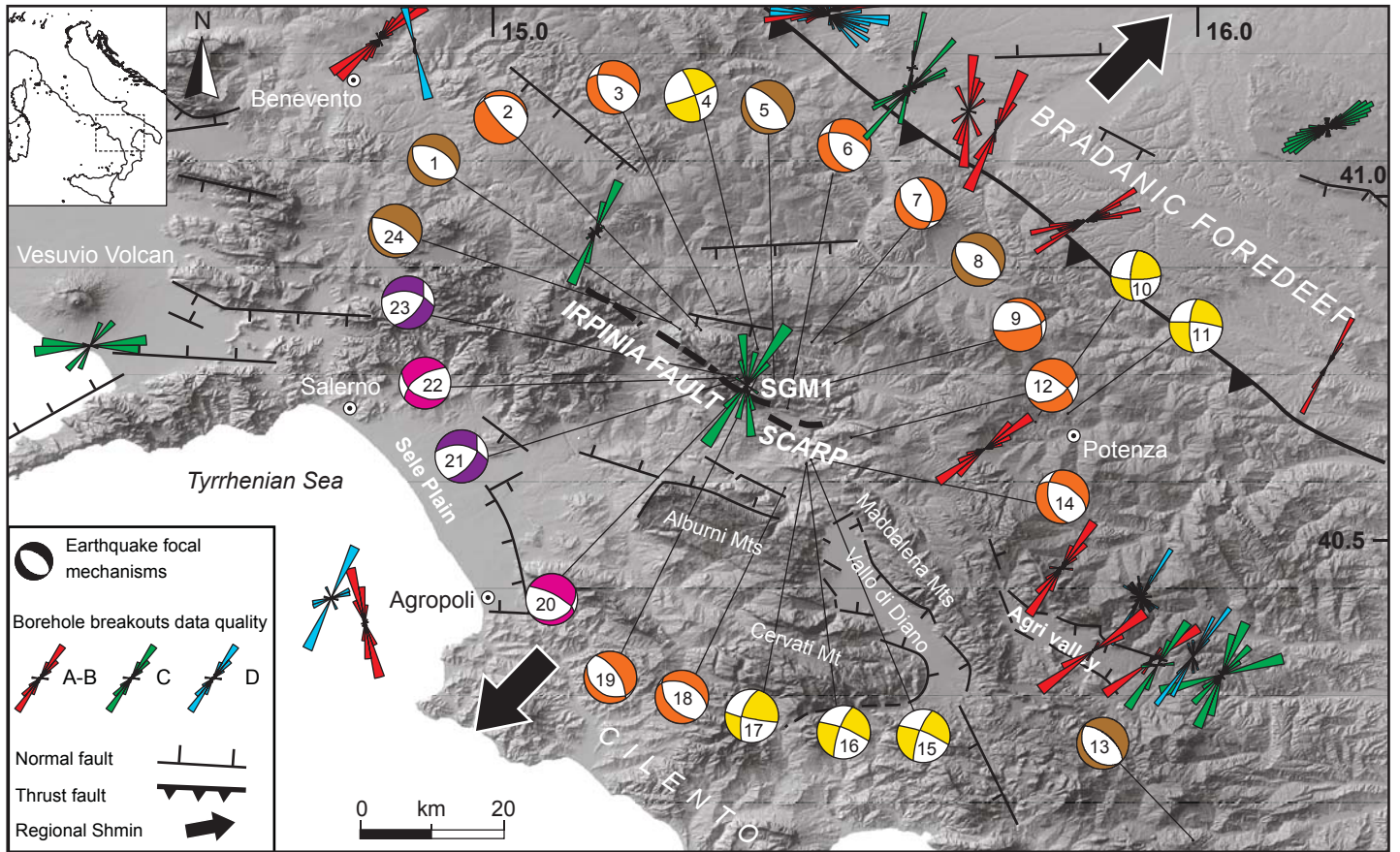


Figure 6

Accepted in

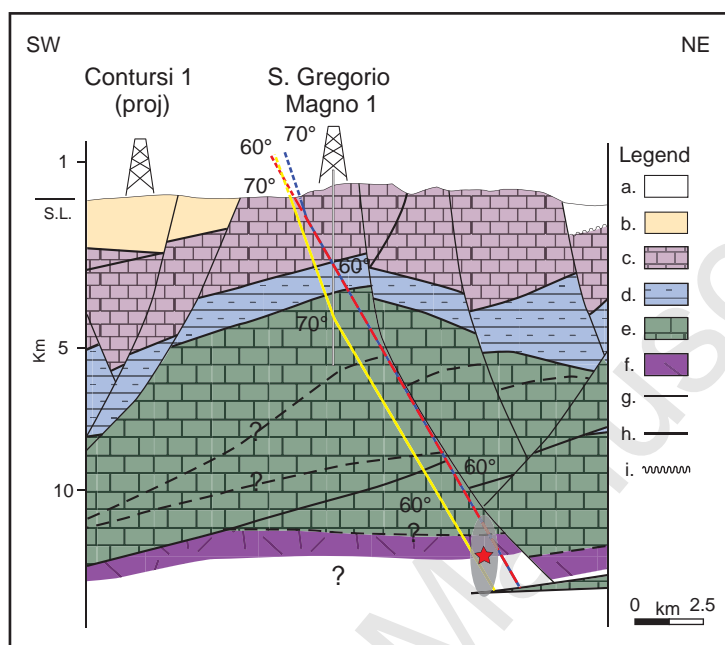


Figure 7

Table 1

Earthquake focal mechanism data (the events are ordered according to figure 6).

Event Number	Event Date (yyyy/mm/dd)	Origin Time	Lat, deg	Lon, deg	Depth (km)	Magnitude	Strike	Dip	Rake	References
1	19801123	18:34	40.724	15.373	10-12	6.9	135	60	-80	a
2	20020102	02:17	40.779	15.417	15.4	2.8	140	75	-80	b
3	20060314	03:15	40.818	15.326	10.5	2.7	155	50	-60	b
4	20060915	17:55	40.766	15.384	16.2	2.4	70	85	-170	b
5	20040224	05:21	40.715	15.407	16.5	3.8	135	25	-90	b
6	20020504	09:41	40.611	15.537	15.8	2.3	160	45	-50	b
7	20061201	15:38	40.775	15.460	15.0	2.7	130	40	-120	b
8	20060717	16:56	40.774	15.490	8.4	2.5	125	40	-90	b
9	20060926	16:29	40.722	15.455	7.8	3.0	80	75	-110	b
10	19900505	07:21	40.775	15.766	15.0	5.7	184	73	13	c
11	19910526	12:26	40.730	15.765	11.0	5.2	183	71	-9	c
12	20020505	06:40	40.373	15.373	21.6	1.9	155	50	-150	b
13	19980909	11:28	40.150	15.947	9.0	5.6	139	29	-83	d
14	20020419	18:06	40.595	15.568	6.0	4.1	170	50	-50	b
15	20020418	21:00	40.588	15.569	10.3	3.0	200	75	-10	b
16	20020418	21:36	40.583	15.573	9.6	2.2	200	80	-10	b
17	20020418	22:58	40.583	15.571	9.5	2.7	100	80	150	b
18	20020526	10:19	40.549	15.534	11.4	2.6	140	45	-70	b
19	19960304	13:04	40.670	15.420	10.0	4.9	111	15	-126	f
20	19960304	13:04	40.670	15.420	8.0	5.1	297	74	-70	e
21	19960717	09:45	40.670	15.400	10.5	3.5	35	55	-140	f
22	19960822	06:47	40.670	15.390	10.0	3.0	115	45	-40	f
23	19960716	12:46	40.670	15.380	12.2	3.4	45	45	-130	f
24	20011209	12:15	40.795	15.287	16.6	3.3	130	20	-80	b

References: a) Boschi et al., 1981; b) Maggi et al., 2009; c) Ekström, 1994; d) Pondrelli et al., 2002; e) Cocco et al., 1999; f) Cucci et al., 2004.

Table 2

Summary of breakout data results of the SGM1 well for each lithological and tectonic unit

Tectonic Unit	Lithological Unit	Depth Units		Breakout Interval		Shmin (°)	standard deviation (°)	Breakout length (m)	Breakout zone number
		Top	Bottom	Top	Bottom				
Alburno-Cervati		40	2280	2000	2075	348	0	75	1
	Dolomia Principale	440	2280	2000	2075	348	0	75	1
Lagonegro II		2280	3377	2325	3275	038	33	365	5
	Galestri	2280	2735	2325	2650	310	14	125	2
	Scisti Silicei	2735	3198	2960	3198	041	7	165	2
	Monte Facito	3198	3377	3200	3275	033	0	75	1
Apulia		3377	5901	3450	5580	007	28	607	14
	Wildflysch	3377	3977	3450	3990	325	15	245	4
	Shallow-Water Carbonates	4085	5901	4090	5580	015	21	362	10